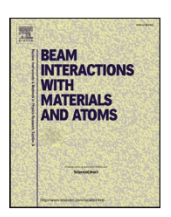
FISEVIER

Contents lists available at ScienceDirect

Nuclear Inst. and Methods in Physics Research B

journal homepage: www.elsevier.com/locate/nimb



First off-line tests and performance of the Notre Dame multi-reflection timeof-flight mass spectrometer



J.M. Kelly^a, M. Brodeur^{a,*}, B. Liu^a, Q. Campagna^{a,b}, C. Gonzales^a, J. Maier^a

- ^a Department of Physics, University of Notre Dame, Notre Dame, IN 46556, USA
- ^b College of William and Mary, Williamsburg, VA 23185, USA

ARTICLE INFO

Keywords:
Ion trap
Multi-reflection time-of-flight mass
spectrometer
Radioactive ion beams

ABSTRACT

A multi-reflection time-of-flight mass spectrometer (MR-TOF) will be a critical component for quickly removing radioactive contaminants produced at the future "N=126 factory" addition to ATLAS at Argonne National Laboratory (ANL). This unique thermalized ion beam facility will employ multi-nucleon transfer reactions to produce very neutron-rich isotopes relevant to the astrophysical r-process. Ion beams produced at this facility will include isobaric contaminants, while precision measurements of such rare isotopes typically require highly purified samples. Hence, to tackle this issue an MR-TOF has been built and commissioned at the University of Notre Dame in an off-line test setup comprising a thermionic source and a Bradbury-Nielsen gate (BNG) to create the ions bunches to be purified. Resolving power above 30,000, with a corresponding efficiency of 35%, has been achieved. Most of the ion beam losses could be the result of the large radial divergence of ion bunches produced by the BNG, hence greater efficiency and resolving power are expected once the MR-TOF is connected to an radiofrequency quadrupole (RFQ) cooler and buncher at ANL.

1. Introduction

The astrophysical rapid-neutron capture (r-) process is responsible for the production of approximately half of all observed elements in the universe [1]. Recently one astrophysical site for this process has been confirmed with the observation of freshly synthesized lanthanides within the kilonova following the GW170817 neutron star merger [2]. This observation gives a strong impetus to bolster the quantity and quality of the experimental nuclear physics data required by r-process abundance calculations.

Over the past few years, several sensitivity studies have been performed to help pin down the most critical nuclei [3]. It has been found that the most sensitive nuclei are located near the closed neutron shells at N=82 and N=126, as well as in the rare-earth region between these shells. While many mass measurements have recently been performed near N=82 [4,5] and in the rare-earth region [6,7], as well as lifetime measurements [8], there is very little experimental efforts near N=126. This stems primarily from the difficulty in producing these heavy nuclei. Indeed, it is found that the cross-section for projectile fragmentation reactions rapidly falls as more protons are removed from the heavy projectile [9,10]. There is, however, an alternate type of reaction, called multi-nucleon transfer (MNT) reactions, which can access this region without suffering from a large drop in cross section

[9,11-13].

The "N = 126 factory" facility currently under development at Argonne National Laboratory (ANL) [14], will make use of such reactions to produce these difficultly accessible nuclei south of $^{208}\mathrm{Pb}.$ The facility will stop the MNT reaction products in a large volume gas catcher. After the extraction from the gas cell, several stages of contamination removal from the radioactive ion beam (RIB) will be required. These will include a mass analyzing magnet with a mass resolving power of $M/\Delta M \approx 1500$ to remove non-isobars and a multireflection time-of-flight (MR-TOF) mass spectrometer to remove isobars. The MR-TOF's advantages are threefold, as it will purify contaminated RIBs [15], it can also perform its own fast and precise mass measurements [16-18], while being elegantly simple in its design and operation [19]. To serve these purposes, such an instrument has been constructed and commissioned off-line at the University of Notre Dame. The off-line experimental set-up, as well as the first commissioning results using a Bradbury-Nielsen gate (BNG) to create the ion bunches will be presented.

2. Components of the MR-TOF off-line setup

The University of Notre Dame MR-TOF has the same electrode dimensions as the ISOLTRAP MR-TOF [20], but uses a different assembly

E-mail address: mbrodeur@nd.edu (M. Brodeur).

 $^{^{\}ast}$ Corresponding author.

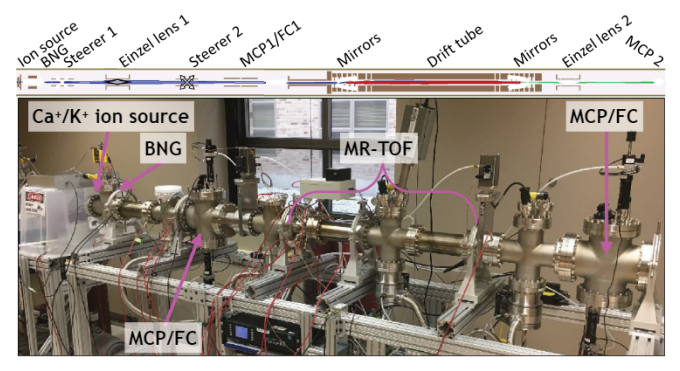


Fig. 1. Top: Schematic of the beam line for the off-line commissioning of the ND MR-TOF (re-scaled for printing). Bottom: Photo of the beam line at the University of Notre Dame.

design [19]. The device includes two electrostatic mirrors bracketing two Einzel lenses and a pulsed drift tube. Each mirror includes five identical electrodes. More details on the MR-TOF structural design and assembly can be found in [19].

The off-line commissioning set-up for the MR-TOF is shown in Fig. 1. It first includes an aluminosilicate ion source [21] that produces, via thermionic emission, alkali ranging from ²³Na to ¹³³Cs in measurable quantities, with ³⁹K being the predominant isotope (see Fig. 2). The ion source is electrically connected to a surrounding electrode floating at a potential of 3.5 kV above the grounded beam line, thereby defining the kinetic energy of the ion beam. Facing the ion source, an anode, typically at a potential of 3.2 kV, is used to extract the ions produced by the source and accelerate them towards a BNG (see Fig. 3).

The BNG is used to produce short ion bunches from the ion source's continuous beam in lieu of an RFQ cooler-buncher [22,23] (nonexistent at the moment of the off-line commissioning) typically used in this application. This is accomplished by rapidly switching ON/OFF/ON the ± 650 V potential applied on two interleaved sets of thin, parallel wires, allowing short bunches of beam to pass unperturbed. The BNG follows the design from [24] with a screen comprising 50 μm diameter wires spaced by 560 μm . Both sets of wires are connected to a fast FET switch that can pulse the ± 650 V potentials to ground with a fall time of ≈ 15 ns and a rise time of ≈ 20 ns. Fig. 2 shows such a pulsed bunch resulting in the production of 20 ns full width half maximum (FWHM) bunches recorded at the micro channel plate detector (MCP) located after the MR-TOF. For all the studies presented, $^{39} \rm K^+$ has been used since it is produced in the greatest abundance.

After the BNG, two sets of x-y steerers correct for beam line misalignment and optimize the on-axis alignment of the ion beam entering the MR-TOF. The two steerers are operated with a common bias of

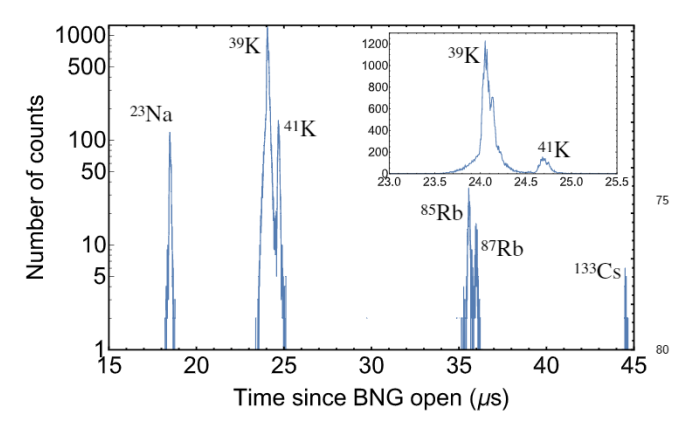


Fig. 2. A time-of-flight spectrum of the various alkali produced by the ion source as recorded on the MCP downstream from the MR-TOF for a $160\,\mathrm{ns}$ opening time of the BNG.

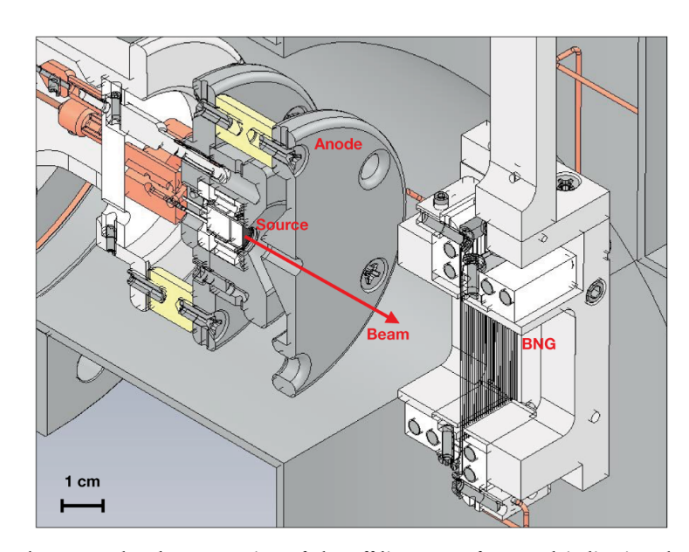


Fig. 3. Rendered cross-section of the off-line setup front end indicating the location of the ion source, anode and Bradbury-Nielsen gate (BNG). Inset shows the thermionic source with a penny for scaling.

1840 V and 100 V, respectively. The bias on the first steerer parallelizes the divergent beam leaving the ion source before it enters the Einzel lens located between the two sets of steerers. The potential applied on the Einzel lens, $-1600\,\mathrm{V}$, has been adjusted to first maximize the transmission through the MR-TOF and then the efficiency after capturing for a given number of loops. A second Einzel lens is located after the MR-TOF to focus the ion beam onto an MCP (see Fig. 1). Due to the short distance travelled by the ion beam exiting the MR-TOF, the transfer efficiency in this section weakly depends on the potential applied (typically $-2500\,\mathrm{V}$) on the second Einzel lens.

Since the ultimate resolving power achievable by the MR-TOF is highly sensitive on the stability of the mirror electrode potentials, 3 EHS high precision modules with floating common ground from ISEG with eight $6\,\mathrm{kV}$ channels each are used to provide the potential for all electrodes including the injection optics.

The BNG FET switch and the 6 kV Belkhe switch connecting to the pulsed drift tube are triggered by an SRS Model DG535 four channel digital delay/pulse generator with a 5 ps delay precision. A duplicate of the latter signal from the pulse generator is used to trigger the acquisition of the pre-amplified signal from the MCP by a SRS SR430 multichannel scaler. Both devices, as well as the ISEG supplies are controlled by a Labview program that enables the scanning of potential of a given electrode and records the corresponding time-of-flight spectra after multiple cycles of measurement.

Finally, the whole system is evacuated by four 300 L/s, turbomolecular pumps backed by a scroll pump. A pressure below 3×10^{-9} mbar is currently achieved at the location of the MR-TOF.

3. Optimization of the MR-TOF

Prior to the optimization of the MR-TOF in the laboratory, a series of simulations optimizing the potential to be applied on the mirror has been performed using the software SIMION [25] and a gradient-ascent code resulting in mass resolving powers in excess of 120,000 after 10 ms [19]. The optimal mirror potential found in the simulations were then used as starting point for the optimization in the laboratory.

The injection optics was first optimized by maximizing the transmission efficiency of the continuous beam from the Faraday cup upstream of the MR-TOF to the Faraday cup downstream. Then the injection optics were further adjusted, with particular attention paid to the steerers, by observing the continuous ion beam profile on the phosphor screen of the two MCPs. The last step of this first stage of optimization consisted of chopping the ion beam at low repetition rate

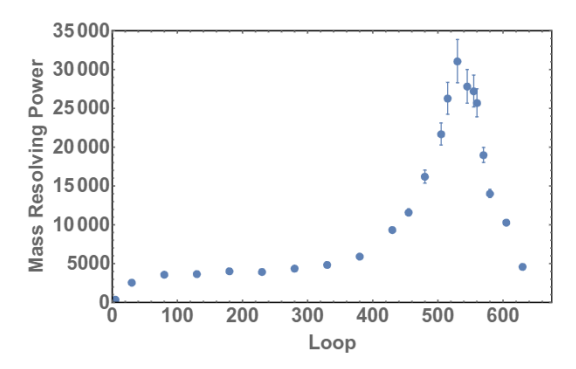


Fig. 4. Mass resolving power (top panel) and transfer efficiency (bottom panel) as function of number of loops.

(1 mHz) with a duty cycle of 50% using the BNG. The deflection voltage of the BNG was then increased until the ion beam was completely deflected 50% of the time, corresponding to a minimum deflection potential of $\pm650\,\rm V.$

For the second stage of optimization, the BNG was set to deflect the ion beam for most of the time except for a short duration of 160 ns, and the repetition rate was increased to 100 Hz, which is the highest repetition rate that the BNG FET switch can accommodate before distorting its output. The system was operated at the highest possible repetition rate to maximize usable beam. The bunch creation method used will then only preserve a fraction $\approx\!160\,\text{ns}/10\,\text{ms}\approx2\times10^{-5}$ of the continuous beam, so an initial ion beam of 1 pA becomes $\approx\!10$ ion/bunch entering the MR-TOF.

After optimizing the transmission of the ion bunch through the MRTOF, the $^{39}\mathrm{K}^+$ bunch was captured using the in-trap lift method [15] for one loop before being released towards the downstream MCP. The capture (16.6 μs from the BNG opening time) and extraction times (16 μs from the capture time) were adjusted such that the $^{39}\mathrm{K}^+$ bunch is located at the center of the MR-TOF for both capture and ejection to minimize their distortion. The mirror electrodes and central drift tube potentials were optimized to minimize the bunch widths. The injection optics and MR-TOF lens electrodes were tuned to maximize the transfer efficiency. Then the number of loops was increased and the MR-TOF tuning process was repeated.

4. Resolving power and efficiency of the MR-TOF

Once the optimization of various mirror electrode potentials was completed, the efficiency and resolving power for increasing number of loop could be determined. The efficiency was calculated from the number of recorded counts in the $^{39}\mathrm{K}^+$ bunch after the given number of loops over the number of recorded counts when shooting through the MR-TOF. The resolving power is calculated as $R = T/2\Delta T$, where T is the average time-of-flight of the $^{39}\mathrm{K}^+$ bunch and ΔT is its full width half

maximum (FWHM). Fig. 4 shows the resolving power as a function of the number of loops, where the maximum mass resolving power obtained is approximately 31,000 after 530 loops ($\approx 8.1 \text{ ms}$), and at 35% efficiency.

Given the ion's current kinetic energy and the system's repetition rate, ions can be held and the time focus tuned for a maximum of about 640 loops, or 9.8 ms, to achieve a higher resolving power of 45,000. However, this comes at the expense of decreased efficiency. It should be noted that the greatest drop is efficiency occurs in the first five loops, at which point only 63% of the ³⁹K+ bunch remain. Recent simulations indicates that this large drop in efficiency as well as the limitation in the resolving power are probably caused by the method of production of the ion bunch using a BNG. Effectively, chopping the continuous beam introduces a large angular spread to the ion bunch, inflating the radial emittance of the bunch as compared to a bunch produced by an RFQ. Simulations are currently underway to further investigate this effect and will be the subject of a forthcoming publication.

Acknowledgement

The authors would like to thank John Brandon from the National Superconducting Cyclotron Laboratory for assembling the Bradbury-Nielsen gate's FET switch. This work was conducted with the support of the National Science Foundation under Grant PHY-1713857, and of the University of Notre Dame.

References

- [1] M. Arnould, S. Goriely, K. Takahashi, Phys. Rep. 450 (2007) 97.
- [2] M.R. Drout, et al., Science 358 (2017) 1570.
- [3] M. Mumpower, R. Surman, G. McLaughlin, A. Aprahamian, Prog. Part. Nucl. Phys. 86 (2016) 86.
- [4] D. Atanasov, et al., Phys. Rev. Lett. 115 (2015) 232501.
- [5] J. Van Schelt, et al., Phys. Rev. Lett. 111 (2013) 061102.
- [6] R. Orford, et al., Phys. Rev. Lett. 120 (2018) 262701.
- [7] M. Vilen, et al., Phys. Rev. Lett. 120 (2018) 262702.[8] J. Wu, et al., Phys. Rev. Lett. 118 (2017) 072701.
- [9] Y. Hirayama, et al., EPJ Web Conf. 109 (2016) 08001.
- [10] T. Kurtukian-Nieto, et al., Phys. Rev. C 89 (2014) 024616.
- [11] R. Kaufmann, R. Wolfgang, Phys. Rev. Lett. 3 (1959) 5.
- [12] J. Galin, D. Guerreau, M. Lefort, J. Peter, X. Tarrago, R. Basile, Nucl. Phys. A 159 (1970) 2.
- [13] Y.H. Kim, Y.X. Watanabe, et al., EPJ Web Conf. 66 (2014) 03044.
- [14] G. Savard, M. Brodeur, J.A Clark, A.A. Valverde, this Issue (2019).
- [15] R.N. Wolf, et al., Nucl. Instrum. Methods Phys. Res., Sect. A 686 (2012) 82.
- [16] F. Wienholtz, et al., Nature 498 (2013) 346.
- [17] T. Dickel, et al., Nucl. Instrum. Methods Phys. Res., Sect. A A777 (2015) 172.
- [18] P. Schury, et al., Nucl. Instrum. Methods Phys. Res., Sect. B 335 (2014) 39.
- [19] B.E. Schultz, et al., Nucl. Instrum. Methods Phys. Res., Sect. B 376 (2016) 251.
- [20] R.N. Wolf, M. Eritt, G. Marx, L. Schweikhard, Hyperfine Interact 199 (2011) 115.
- [21] HeatWave Labs, http://www.heatwavelabs.com/.
- [22] A.A. Valverde et al., this Issue (2019).
- [23] F. Herfurth, et al., Nucl. Instrum. Methods Phys. Res., Sect. A 469 (2001) 2.
- [24] T. Brunner, et al., Int. J. Mass Spectrom. 309 (2012) 97.
- [25] D.A. Dahl, Int. J. Mass Spectrom. 3 (2000) 200.